†Electronic Supplementary information (ESI) available: [Details of sections A1-A2 and Figures S1-S8]

Single-step green synthesis of imine-functionalized carbon spheres and their application in uranium removal from aqueous solution

Shashi Prabha Dubey[a,b], Amarendra Dhar Dwivedi[b], Mika Sillanpää[b], Young-Nam Kwon[a,*], Changha Lee[a,*]

[a] School of Urban and Environmental Engineering, Ulsan National Institute of Science and Technology (UNIST), 100 Banyeon-ri, Eonyang-eup, Ulju-gun, Ulsan 698-805, Republic of Korea
[b] Laboratory of Green Chemistry, LUT Chemtech, Lappeenranta University of Technology, Sammonkatu 12, 50130 Mikkeli, Finland

[*]Corresponding Authors
Tel: +82-52-217-2810 (Y.-N. Kwon); +82-52-217-2810 (C. Lee)
E-mail: kwonyn@unist.ac.kr (Y.-N. Kwon); clee@unist.ac.kr (C. Lee)

A1. Comparative characterization results for gCSs and peCSs

Supplementary Fig. S1a shows the FTIR spectra of gCS functional groups to correlate the significant peaks in both samples. A broad peak at 3369 and 2929 cm^{-1} could be associated with -OH and -CH stretching vibrations. The band observed at 1695 cm^{-1} may be due to C=O stretching vibrations. Other bands at 1654, 1605 and 1511 cm^{-1} could be attributed to the presence of C=C stretching vibrations.
Supplementary Fig. S1b shows prominent Raman peaks of the gCS sample. The difference in intensity between the G peak (more intense) and the D peak (less intense) was greater in the peCS than the gCS sample. Furthermore, the intensity ratio of the D and G bands (I_D/I_G) was lower in the peCS sample (0.901) than the gCS sample (0.923), indicating fewer defects and a more extensive sp^2-bonded carbon network in the peCS samples than the gCS samples.
Supplementary Fig. S2a shows the XRD pattern of gCSs. It exhibited two peaks (indexed as (002) and (100) phases) of amorphous carbon, similar to those observed in the synthesized peCSs samples.
Supplementary Fig. S2b shows the N_2 adsorption/desorption curve of the gCS sample. The specific surface area measured from the BET equilibrium was 29.56 $m^2.g^{-1}$ for gCSs, which was higher than that for the peCS sample (16.77 $m^2.g^{-1}$). However, the peCSs featured a larger pore size (8.31 nm) than the gCSs did (6.78 nm).
Supplementary Fig. S3 shows the XPS survey spectra of the gCS sample. The C1s and O1s peaks are observed at 284.88 and 532.78 eV, respectively. For the gCSs, no peak was detected for N 1s.
Supplementary Fig. S4a and b shows the TGA and DSC curves, respectively, of the gCS sample in air and N_2 atmosphere. Similar decomposition/combustion processes were observed for the gCS and peCS samples.

A2. Kinetic and isotherm study

The kinetic and isotherm equations used to model the experimental data are presented in Table S1.

Table S1. Modelling equations

Adsorption parameters	Equations used
Kinetic models	
Pseudo first order[1]	$q_t = q_e - \left(\frac{q_e}{10^{k_1 t/2.303}}\right)$
Pseudo second order[2]	$q_t = \frac{q_e^2 k_2 t}{1 + q_e k_2 t}$
Intra-particle diffusion[3]	$q_t = k_{ipd}\sqrt{t} + C$
Isotherm models	
Langmuir[4]	$q_e = \frac{Q_m k_l C_e}{1 + k_l C_e}$
Freundlich[5]	$q_e = k_f C_e^n$
Dimensionless separation factor[6]	$S_f = \frac{1}{1 + k_l C_0}$

Kinetic model parameters:
q_e and q_t ($mg.g^{-1}$) are the adsorption capacities at equilibrium and time t, respectively; k_1 (h^{-1}) is the pseudo-first-order rate constant, k_2 is the rate constant of pseudo-second-order adsorption ($g.mg^{-1}.h^{-1}$), k_{ipd} ($mg.g^{-1}.\sqrt{h^{-1}}$) is the intraparticle diffusion rate constant, and C is the intercept of plot (q_t and $\sqrt{t}$). MicroCal Origin (Origin 8) software was used to find the best fit of the kinetic and equilibrium data.

Isotherm model parameters:
q_e ($mg.g^{-1}$) is the amount of adsorbate adsorbed per gram of adsorbent, C_e is the equilibrium concentration of adsorbate ($mg.L^{-1}$), Q_m is the monolayer adsorption capacity ($mg.g^{-1}$), and k_l is the Langmuir constant related to the free energy of adsorption/desorption ($k_l \propto e^{-\Delta_{ads}G/RT}$). k_f and n are empirical constants in Freundlich isotherm.
Dimensionless separation factor: k_l is the Langmuir constant, C_0 is the initial concentration of adsorbate and S_f indicates the reliability of the indicator of the isotherm.

Fig. S1: (**a**) FTIR and (b) Raman spectra of peCS and gCS samples

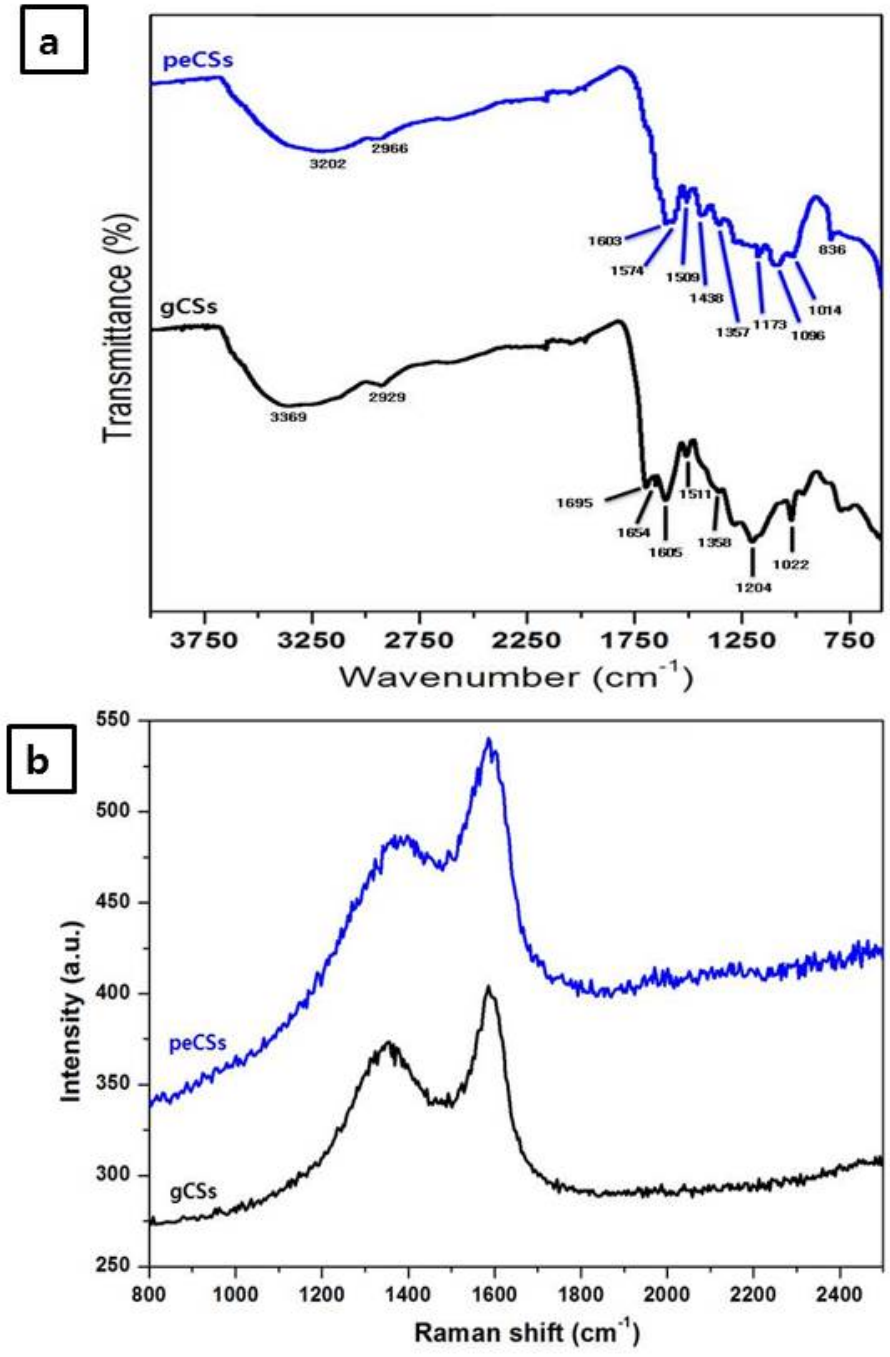

Fig. S2: **(a)** XRD patterns and **(b)** N_2 adsorption/desorption curves of peCS and gCS samples

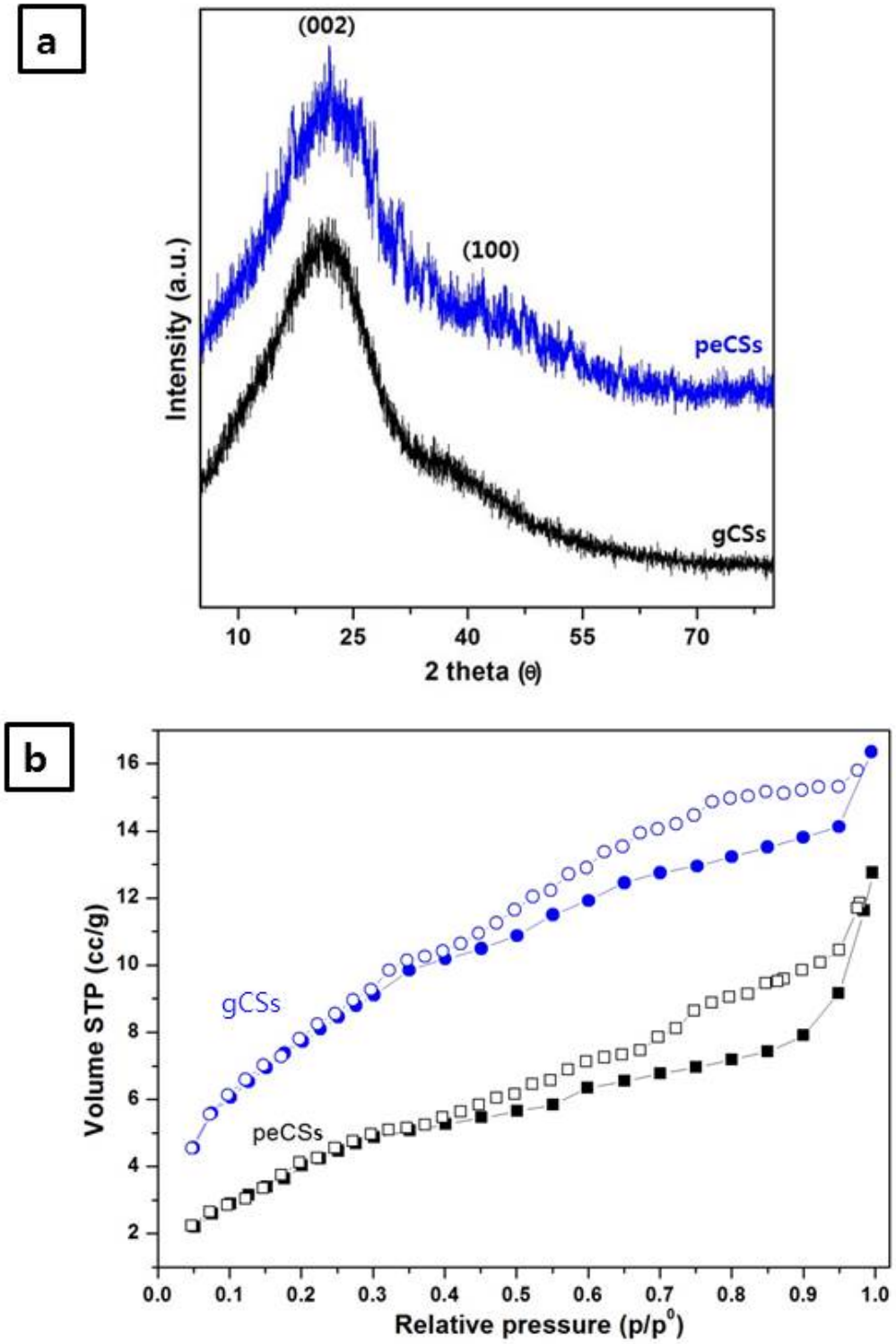

Fig. S3: XPS survey spectra of native gCSs and gCSs after adsorption

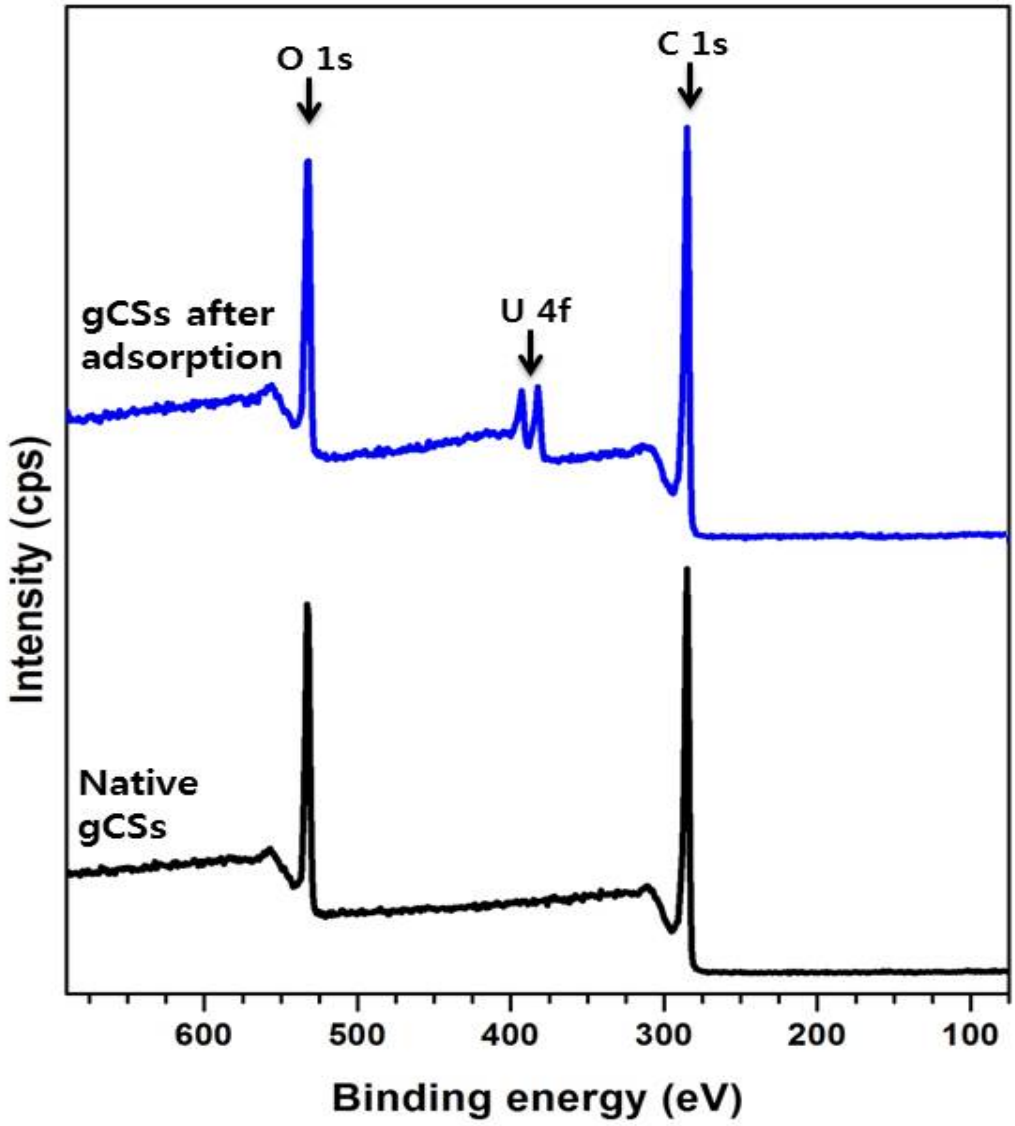

Fig. S4: **(a)** TGA and **(b)** DSC curves of gCS samples in air and N_2 atmosphere

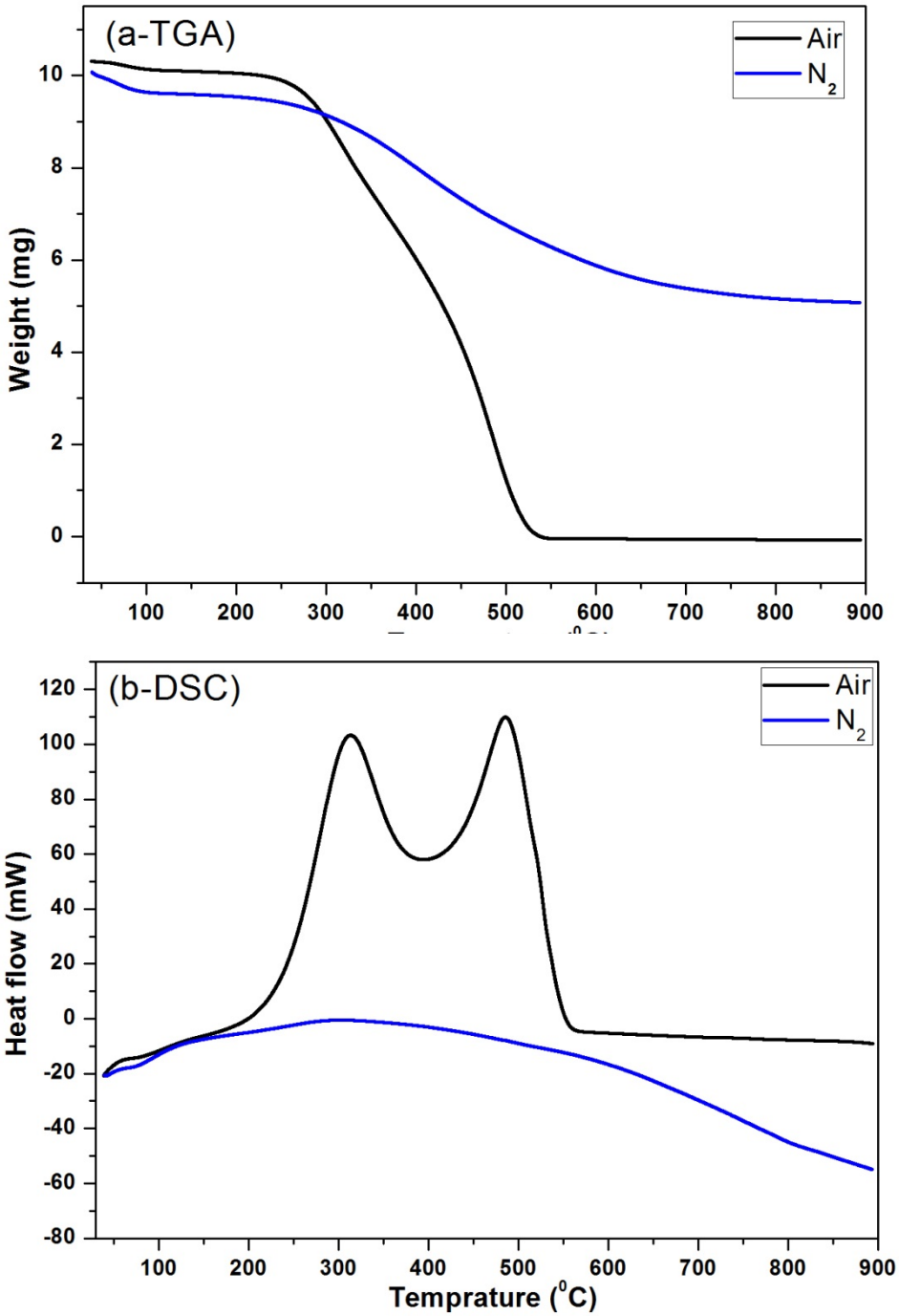

Fig. S5. Variation of the ζ-potential of peCSs with pH

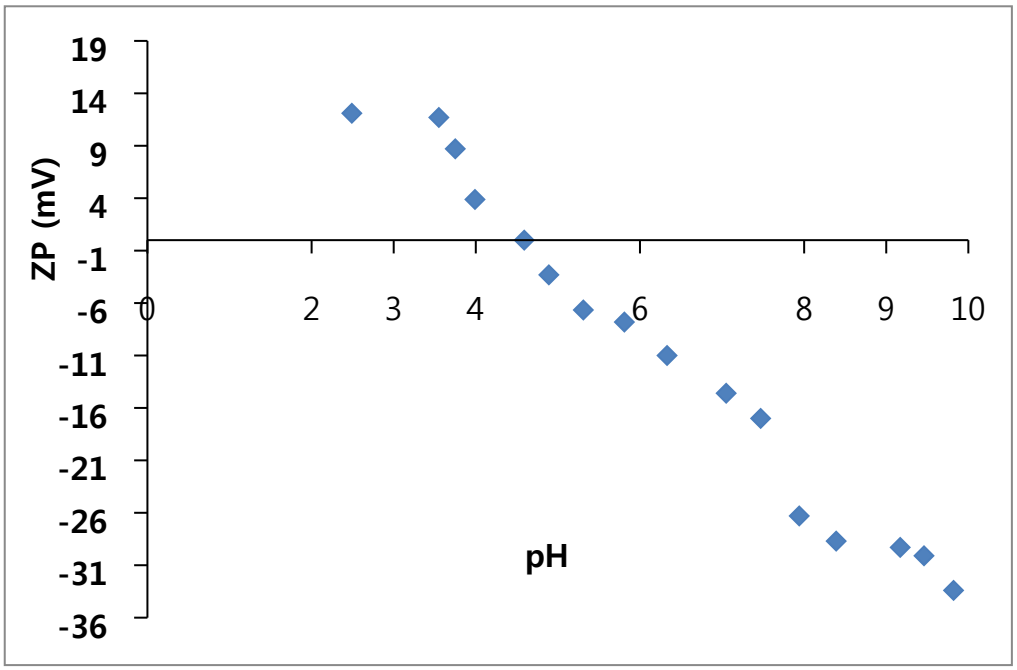

Fig. S6: Speciation of U(VI) as a function of pH (calculated by MINEQL+ 4.6 using constants from ref. 38); $[U(VI)]_0 = 5\ mg.L^{-1}$

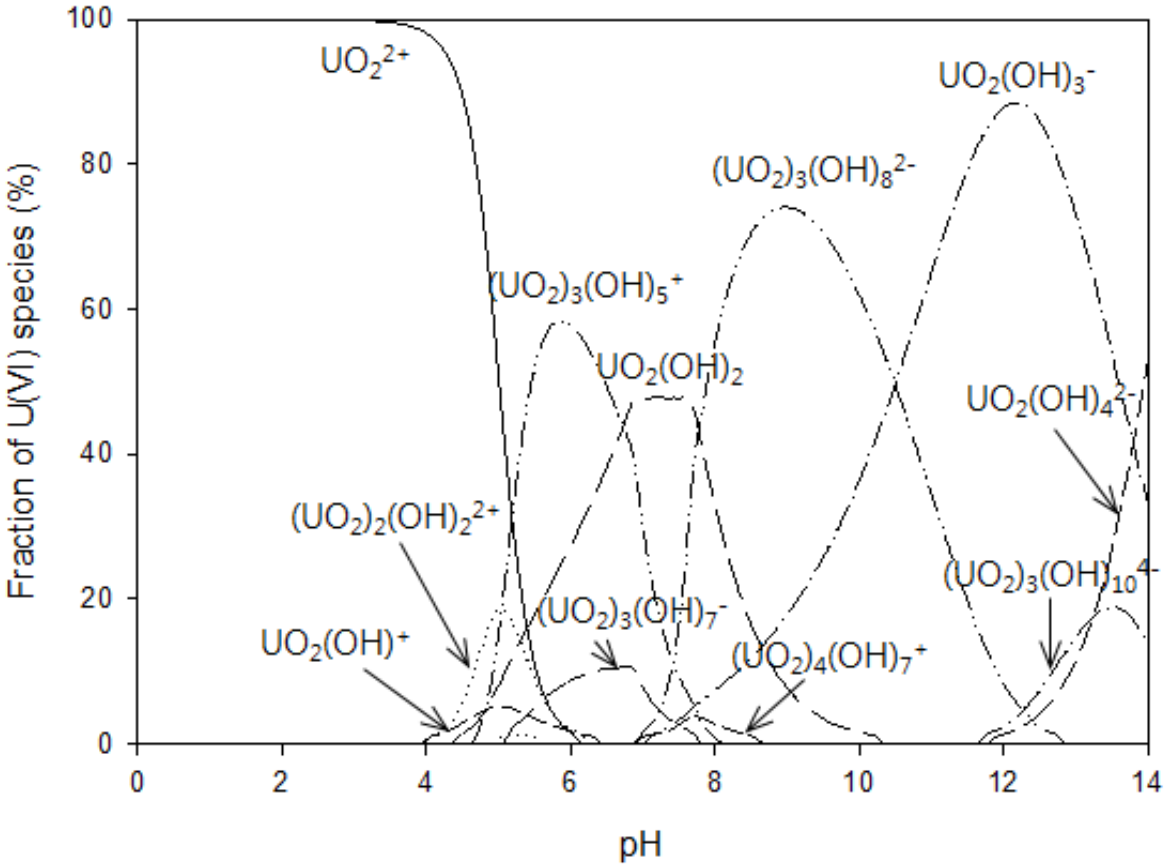

Fig. S7: U(VI) removal efficacy by peCSs, gCSs and PAC: $[\text{Adsorbent dose}]_0$ = 5 mg, $[U(VI)]_0$ = 5 $mg.L^{-1}$, U(VI) volume = 20 mL, reaction time = 6 h, pH = 4

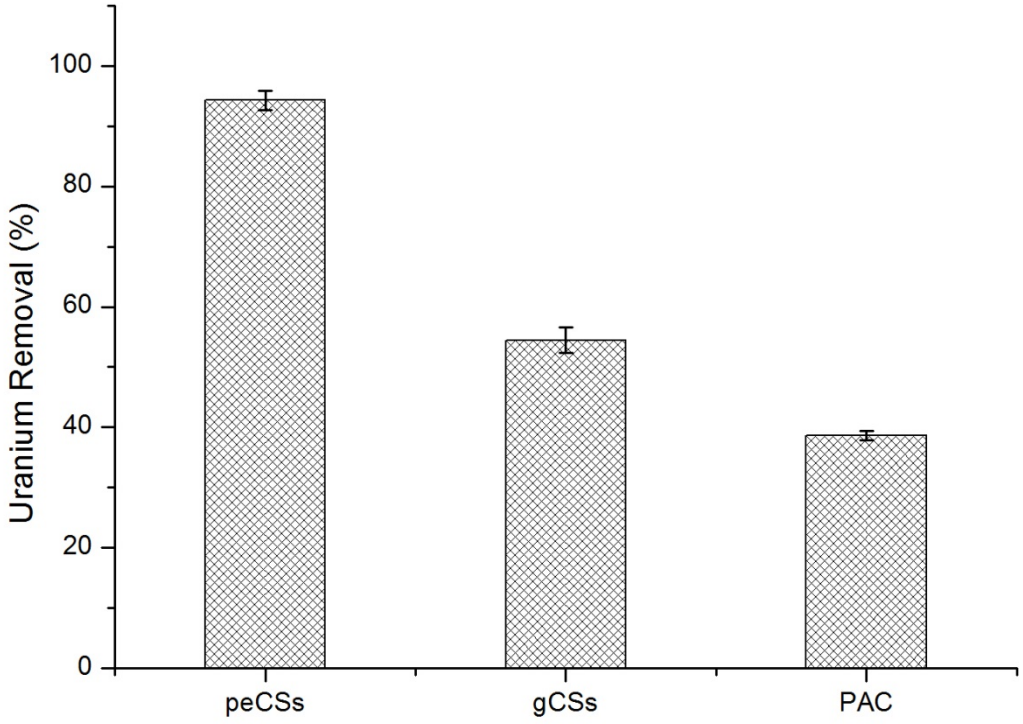

Fig. S8: Intraparticle diffusion plots for U(VI) adsorption on peCSs, gCSs and PAC

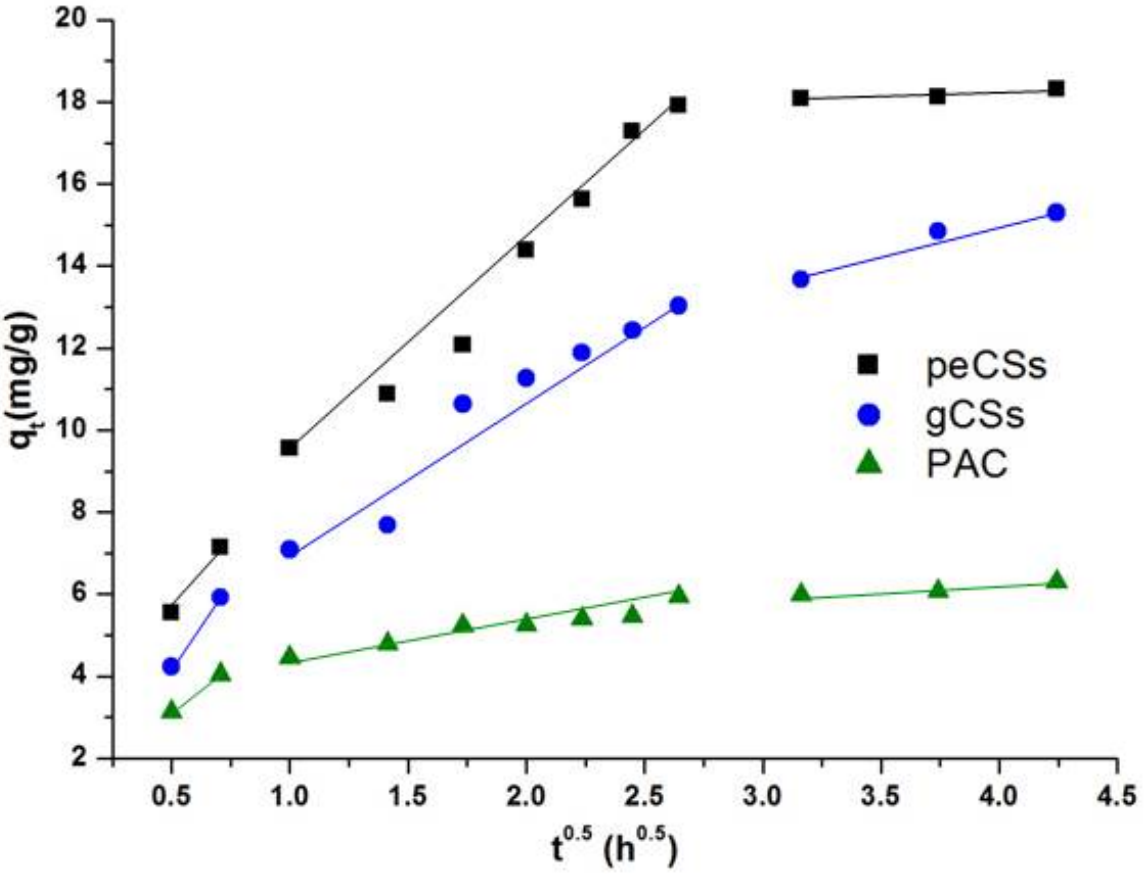

References

1. S. Lagergren, *Kungliga Svenska Vetenskapsakademiens Handlingar,* 1898, **24**, 1–39.
2. Y.S. Ho, G. McKay, D.A.J. Wase and C.F. Foster, *Adsorp. Sci. Technol.,* 2000, **18**, 639–650.
3. V. Srihari and A. Das, *Desalination,* 2008, **225**, 220-234.
4. I. Langmuir, *J. Am. Chem. Soc.,* 1918, **40**, 1361–1367.
5. H.M.F. Freundlich, *J. Phys. Chem.,* 1906, **57**, 385–470.
6. Y.S. Ho, C.T. Huang and H.W. Huang, *Process Biochem.,* 2002, **37**, 1421-1430.